Paper accepted for presentation at 2009 IEEE Bucharest Power Tech Conference, June 28th - July 2nd, Bucharest, Romania

A Modified Nonlinear Damping of Zero - Dynamics via Feedback Control for a STATCOM

Youngseong. Han, Young O. Lee, *Student Member, IEEE* and Chung C. Chung†, *Member, IEEE*

***Abstract*--Recently linearization via feedback control law for a STATCOM to minimize the internal dynamics oscillations was proposed. The ripples of the internal dynamics correspond to the oscillation of the current ripple on the DC side capacitor so that it affects the lifecycle of the capacitor. In this paper, a modified nonlinear damping of zero dynamics via feedback control for a STATCOM is proposed. The proposed nonlinear feedback controller improves the stability of the internal dynamics. The controller gives the damping on zero-dynamics via the nonlinear feedback controller optimized at each operating point. It guarantees internal stability in all operation regions by moving the poles of the internal dynamics away from the imaginary axis. This effect is validated through the root locus analysis. Simulation results show that the oscillation of the internal dynamics is effectively reduced using the averaged and the topological model.**

***Index Terms*--input-output linearization, internal (zero) dynamics, nonlinear damping, STATCOM**

I. Introduction

STATCOM (Static Synchronous COMpensator) compensates for reactive power, regulates voltage and stabilizes power flow. It has become popular due to its attractive performance and operating characteristics [1]. The STATCOM is a highly nonlinear system. Through the input-output linearization method, nonlinear system gets a linear behavior by separating the internal dynamics from it. This method allows the nonlinear system to be controlled by linear control theory. Multivariable feedback linearization of STATCOM systems have been studied in [2]-[4]. Through input-output linearization, nonlinearity of the system can be canceled and one dimensional zero dynamics is obtained. On the other hand, the single-input-single-output linearization proposed by [5], [6] results in a two dimensional internal dynamics which includes the active current, I_d and DC voltage, V_{dc}. These are unobservable from the output and do not affect the output, the reactive current, I_q. The control methods for voltage and transient stability have been research topics for STATCOM [7], [8]. However the problem about instability of the internal dynamics of the STATCOM has not been extensively researched. Unstable internal dynamics have been researched in terms of tracking performance [9], [10] and stabilization of closed-system with controllers [11].

A nonlinear controller based on input-output linearization via feedback was proposed to provide better performance than a standard constant parameter PI controller [5]. Although the stability of the closed-loop system is guaranteed on the whole operating range, large internal dynamics oscillation exists. The ripples of the internal dynamics correspond to the oscillation of the current ripple on the DC side capacitor so it affects the lifecycle of the capacitor. The unstable internal dynamics can be stabilized by using a large DC side capacitor so that the resonant reference is assigned out of operating point. However, it is not economical to use such a large one. Linearization via feedback control law for a STATCOM to minimize the internal dynamics oscillations was proposed [6]. The nonlinear feedback controller takes into account the dynamics of I_d and V_{dc} of a STATCOM system. The I_d derivative term with respect to time multiplied by a constant gain was added to the control law. The controller decreases the I_d and V_{dc} oscillation at some operating point by moving the poles of the internal dynamics. However, this controller cannot guarantee the system to be internally stable at every operating point.

In this paper, a nonlinear feedback controller that guarantees internal stability at every operating point is investigated. The controller also has a derivative term of the I_d in the control law. Unlike the controller in [6], the term is multiplied by variable gains according to the operating points. It guarantees internal stability in all operation regions. Further by moving the poles of the internal dynamics away from the imaginary axis it brings more improved performances such as settling time, T_s and percentage overshoot (%OS) of I_d and V_{dc} than the controller in [6]. All results are analyzed in the view of the root locus at all operating points. The response time is validated by simulation using the averaged model as well as the topological model. Simulation results show that the oscillation of the internal dynamics is effectively reduced. The topological model of STATCOM accurately describes the

This work was supported by Hyosung Co., Korea. It was also in part supported by the Brain Korea 21 Project in 2008.

Y. Han is with Dept. of Electrical Engineering, Hanyang University, Seoul 133-791, and also with Power & Industrial Systems R&D Center, Hyosung Co., Gyeonggi-Do 431-080, KOREA(e-mail: yshan@hyosung.co.kr)

Y. O. Lee is with Dept. of Electrical Engineering, Hanyang University, Seoul 133-791, KOREA (e-mail: foryou5252@hotmail.com)

C. C. Chung is with Dept. of Electrical and Biomedical Engineering, Hanyang University, Seoul 133-791, KOREA (+82-2-2220-1724; fax:+82-2-2291-5307; e-mail: cchung@hanyang.ac.kr)

†: Corresponding Author

978-1-4244-2235-7/09/$25.00 ©2009 IEEE

successive configuration of the STATCOM in the MATLAB/ Simulink environment based on the model with 345kV, 100MVA, 24pulse [5].

This paper is organized as follows. In section Ⅱ, the configuration of the STATCOM is introduced. With this configuration, the input-output linearization approach is presented in section Ⅲ. In section Ⅳ, two nonlinear feedback controllers are presented. The comparison of results between the two controllers is investigated through root locus analysis at the operating point in section Ⅴ. Performances in time domain are presented in section Ⅵ and conclusions follow in section Ⅶ.

II. STATCOM MODEL

The STATCOM produces an alternating voltage source in phase with the transmission line voltage and is connected to the line through an inductance in series. It converts the DC voltage at its input terminal into a three-phase set of output voltages using a voltage source inverter [12]. The system controls voltage, current as well as reactive power and enhances the voltage stability by generating or absorbing the reactive power.

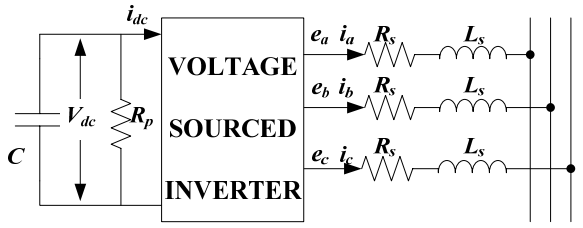

Fig. 1. Equivalent circuit of STATCOM

Fig 1 shows the equivalent circuit of STATCOM. The resistance in series with the ac-lines, R_s, represents conduction losses between the inverter and transformer. The inductance in series with the ac-lines, L_s, represents the leakage of the actual power transformers and the resistance in shunt with the capacitor, R_p, is the switching losses in the inverter [13].

$$\begin{bmatrix} \frac{dI_d'}{dt} \\ \frac{dI_q'}{dt} \\ \frac{dV_{dc}'}{dt} \end{bmatrix} = [A] \begin{bmatrix} I_d' \\ I_q' \\ V_{dc}' \end{bmatrix} - \begin{bmatrix} \frac{\omega |v'|}{L'} \\ 0 \\ 0 \end{bmatrix} \quad (1)$$

where

$$[A] = \begin{bmatrix} -\frac{R_s'\omega}{L'} & \omega & \frac{k\omega\cos(\alpha)}{L'} \\ -\omega & -\frac{R_s'\omega}{L'} & \frac{k\omega\sin(\alpha)}{L'} \\ -\frac{3}{2}kC'\omega\cos(\alpha) & -\frac{3}{2}kC'\omega\sin(\alpha) & -\frac{\omega C'}{R_p'} \end{bmatrix}$$

For the STATCOM controller type, type 1 and type 2 inverter controllers have been used. For the type 1 control method, the phase angle of the voltage, α and the factor, k, that is a factor for the inverter relating the DC voltage to the peak voltage on the AC side are the control inputs. For the type 2 control method, α is the only control input. In this paper, the type 2 inverter controller is considered. Based on this structure, a mathematical averaged model of STATCOM is obtained as (1).

In this paper, STATCOM model is based on the 345kV, 100MVA system and its system parameters are listed in TABLE I.

TABLE I
SYSTEM PARAMETERS USED IN SIMULATIONS

Parameter	Value	unit
AC system voltage (line to line)	345	kV
Converter rate	100	Mvar
R_s'	0.0071	pu
L'	0.15	pu
R_p'	727.5846	pu
C'	2.78	pu
k	0.6312	

III. STATCOM SYSTEM INPUT-OUTPUT LINEARIZATION

Through input-output linearization, the nonlinearity of the system can be canceled. Then we can proceed to solve the I_q tracking control problem using linear control theory [14]. STATCOM system has nonlinearity due to sinusoidal term of α.

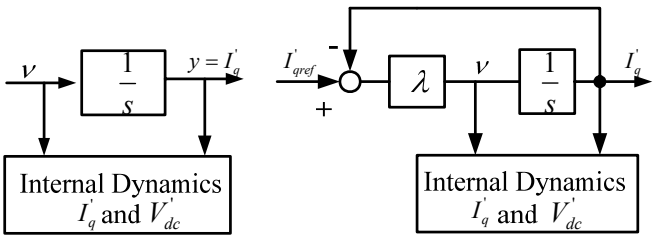

(a) (b)

Fig. 2. (a) Input-output linearized system (b) closed-loop control system

The relative degree of the STATCOM model (1) is one. The relation between new input, v and output, I_q, is represented as an integrator of degree 1. The 2-dimension subsystem includes the internal dynamics, I_d and V_{dc}, as shown in Fig. 2(a). The internal dynamics is unobservable from the output, I_q and does not affect the output [14]. The closed loop system in I_q regulator mode is shown in Fig. 2(b).

$$\alpha = \sin^{-1}\left\{ \frac{L'(\omega_b I_d' + \frac{R_s'\omega_b}{L'} I_q' + v)}{k\omega_b V_{dc}'} \right\} \quad (2)$$

where $v = \lambda\left(I_{qref}' - I_q'\right)$.

The control input, α, can be described as (2). In this paper, a proportional (P) controller is considered for the simple expansion of the equation. The gain of the P controller is λ.

$$\begin{bmatrix} \frac{dI_d^{'}}{dt} \\ \frac{dI_q^{'}}{dt} \\ \frac{dV_{dc}^{'}}{dt} \end{bmatrix} = [A_F] \begin{bmatrix} I_d^{'} \\ I_q^{'} \\ V_{dc}^{'} \end{bmatrix} - [B_F] \begin{bmatrix} v \\ \\ I_{qref}^{'} \end{bmatrix} \tag{3}$$

The input-output linearized system equation can be arranged as (3). The exact mathematical model of this system is in Appendix. The linear controller in Fig. 2(b) can make the input-output linearized system track the desired trajectory, I_q. But the controller does not have influence to the stability of the internal dynamics, I_d and V_{dc}. The ripples of the internal dynamics correspond to the oscillation of the current ripple on the DC side capacitor. The large %OS and slow settling time of the current ripple can shorten lifecycle of the capacitor. The stability of the internal dynamics will be discussed in the next section.

IV. Controller Design

In this section, two nonlinear feedback controllers are introduced for the stabilization of the internal dynamics.

A. Nonlinear Feedback Controller 1

$$\alpha_1 = \sin^{-1}\left\{ \frac{L^{'}(\omega_b I_d^{'} + \frac{R_s^{'}\omega_b}{L^{'}} I_q^{'} + \delta \frac{dI_d^{'}}{dt} + v)}{k\omega_b V_{dc}^{'}} \right\} \tag{4}$$

where $v = \lambda\left(I_{qref}^{'} - I_q^{'}\right)$.

Petitclair *et al.* designed the nonlinear feedback controller (4). The I_d derivative term with respect to time multiplied by constant gain, δ, was added to the control law (2) [6]. This controller makes the poles of the internal dynamics moved. It was shown that the poles of the internal dynamics with large magnitude of δ are moved further to the left half plane (LHP) than with small one [6], but this conclusion depends on the system parameters. For the parameters in TABLE I, the internal dynamics becomes more stable as the magnitude of δ becomes smaller at some operating points. The internal dynamics becomes unstable even in the inductive mode for large values of δ.

B. Nonlinear Feedback Controller 2

There is little phase margin near the system resonant frequency in the inductive region. Schauder constructed the synthesized feedback controller in order to improve the damping in the inductive region [15]. In [15] the feedback quantity 'q' was determined as (5). .

$$q = \left[i_q^{'} - i_{q0(critical)}{}^{'} \right] \left(\frac{s}{1+sT} \right) V_{dc}^{'} \tag{5}$$

where $i_{q0(critical)}{}^{'} = \frac{2}{3kC^{'}} V_{dc}^{'}$

The synthesized feedback has the effect of relocating the open loop transfer function zeroes so that the closed loop root locus is always in the LHP, indicating stable operation. In this paper, a new modified nonlinear feedback controller 2 (6) is constructed.

$$\alpha_2 = \sin^{-1}\left[\frac{L^{'}\left\{ \omega_b I_d^{'} + \frac{R_s^{'}\omega_b}{L^{'}} I_q^{'} + g\left(I_q^{'} - I_{qx}^{'}\right)\frac{dI_d^{'}}{dt} + v \right\}}{k\omega_b V_{dc}^{'}} \right]$$

$$\left(I_{qx}^{'} = \frac{2}{3kC^{'}} V_{dc}^{'} \right) \tag{6}$$

The controller output, α_2, has added term compared to (2). It has a variable gain $g(I_q^{'}\text{-}I_{qx}^{'})$ which is multiplied by $dI_d^{'}/dt$ term. g is constant real number and I_{qx} is the value that varies depending on the V_{dc}. The variable gain makes the poles of the internal dynamics move far from the imaginary axis compared with the controller (4). Within a reasonably bounded g, the internal stability is guaranteed at all operating points irrespective of g. The basic idea of designing the added term in (6), $g(I_q^{'}\text{-}I_{qx}^{'})$ is similar to it in [13], but the purpose and injected position is clearly different. The controller (6) is for internal stability while the controller in [15] is for the damping of the response.

V. Analysis of the Internal Dynamics through Root-Locus Analysis

When input-output linearization is performed, there are 3 poles at each operating point in the closed loop system. The real pole is the same as the P controller gain, λ and the others are internal dynamics poles that are independent of λ. However, the inclusion of the (nonlinear) damping term in the control input, α is not the control law for exact input-out linearization. Through the analysis of the closed-loop system poles, the effects of the two nonlinear feedback controllers introduced in Sec. IV are compared

A. Internal Dynamics with Controller 1

Fig. 3 shows the poles of the input-output linearized closed loop system according to the operating points within the interval -1[pu] to 1[pu] for each δ (gain of the Id derivative with respect to time). If δ is not zero, the real pole is not exactly same as the controller gain but stays near within ±0.5 range.

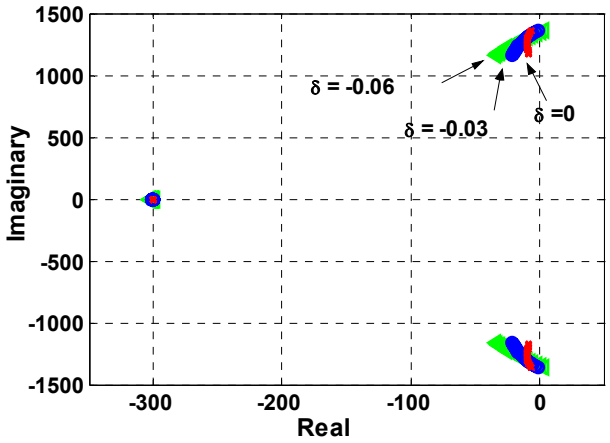

Fig. 3. Root locus of the controller 1 according to the variation of δ

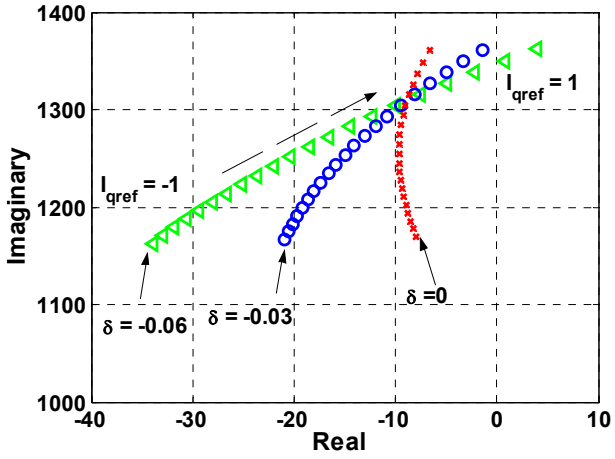

Fig. 4. Root locus of the controller 1 according to the variation of δ (Fig. 3 zoom in)

Fig. 4 is the zoom in of Fig. 3. If δ is determined as a positive real number then the poles are in right half plane (RHP). We can estimate the time response characteristics of the internal dynamics, I_d and V_{dc}, because the magnitude of the real pole is 5 times larger than that of the complex conjugate poles. When the operating points are in -1.0 - 0.6[pu], the internal dynamics has large real part of the complex poles with small δ. Therefore, the settling time, Ts, becomes faster and %OS becomes smaller. On the contrary when the operating points are 0.6 - 1.0[pu], the internal dynamics becomes unstable at some operating points with δ = -0.06. Moreover, Ts becomes increased and %OS becomes larger with decreased δ. We can conclude that variable δ is needed to improve and stabilize the internal dynamics' time response characteristics at each operating point.

Fig. 5 shows the root locus when the two times capacity of the original capacitor is used. If we use the larger DC side capacitor, the internal dynamics becomes stable at all operating points, but this method is not economical.

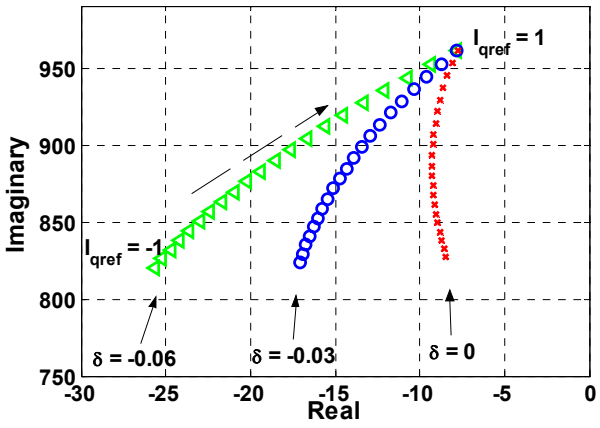

Fig. 5. Root locus of the controller 1 according to the variation of δ with double magnitude of the DC side capacitor

B. *Internal Dynamics with Controller 2*

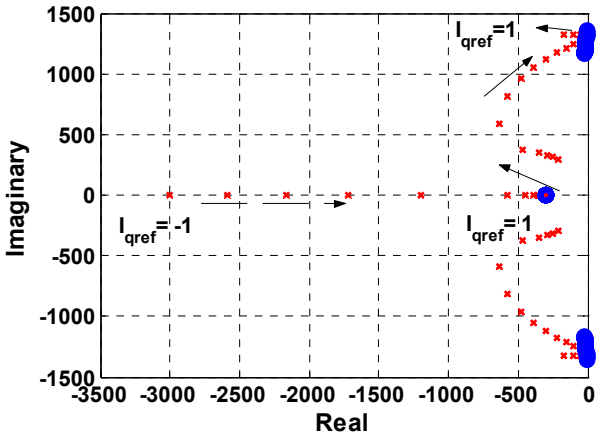

Fig. 6. Root locus comparison between controller 1 and controller 2

Fig. 6 shows the root locus comparison between the systems with controller 1 and controller 2. The internal dynamics of the system with controller 2 becomes stable within a reasonably bounded g for all operating points. When the controller 2 is applied, the real pole is not exactly the same as the controller gain and varied within large range according to the operating points and not always larger than the complex conjugate poles, but we observed that settling time and %OS are improved although we cannot estimate them with the location of the complex poles.

The real part of the poles of the internal dynamics with the controller 2 is 1.5 - 129 times larger than the one with the controller 1. Thus we can estimate T_s and %OS of I_d and V_{dc} will be improved if controller 2 is applied to the system, i.e. with variable gain at each operating points.

VI. Performance of the Nonlinear Feedback Controllers

A. Simulation Results using an Averaged Model

Comparison of the performance of the proposed control strategies is performed through simulation studies using a STATCOM averaged model implemented in MATLAB/ Simulink. The model does not include power electronic switching devices but only STATCOM dynamics (1). This model is used for verifying the control strategy in ideal environment. Control specifications are the following: T_s<16[ms], e_{ss} <5[%] and %OS <10[%].

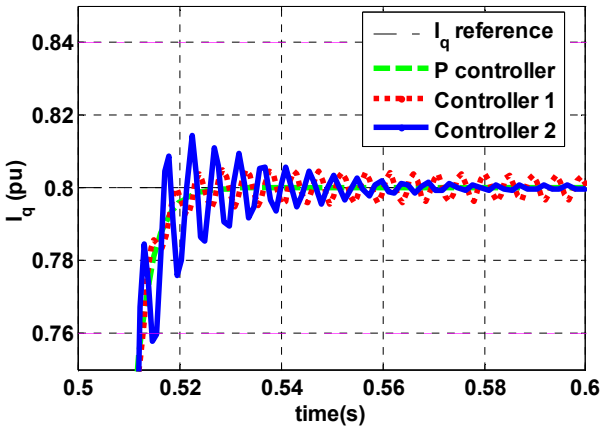

Fig. 7. Reactive current tracking performance in inductive mode

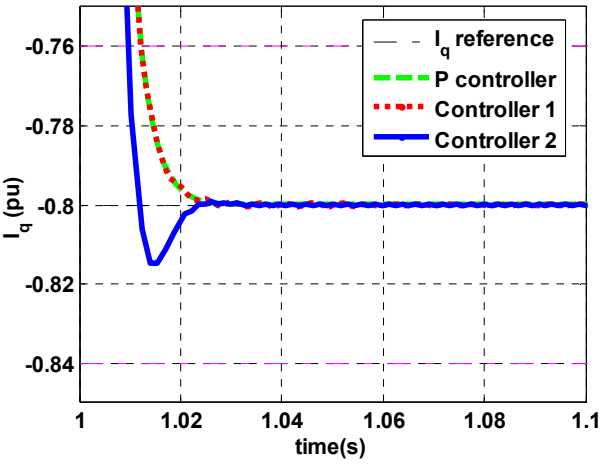

Fig. 8. Reactive current tracking performance in capacitive mode

Firstly, the I_q tracking performance is compared in the case of the reference are 0.8[pu] (Fig. 7) and –0.8[pu] (Fig. 8). The period is set at 0.5[s]. The performance specifications are all satisfied in both cases. The P controller's performance is the best. The controller 2 has the largest %OS and continuous oscillations.

If we only compare the reference tracking performance, it seems like the P controller is the best one. However, it is necessary to investigate the internal dynamics which is unobservable. Fig. 9 shows the I_d oscillations of the 3 controllers at operating point 0.8[pu] and Fig. 10 shows at –0.8[pu].

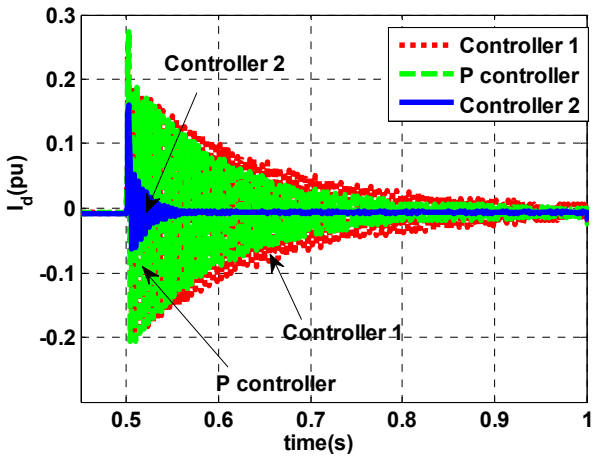

Fig. 9. Active current oscillation comparison in inductive mode

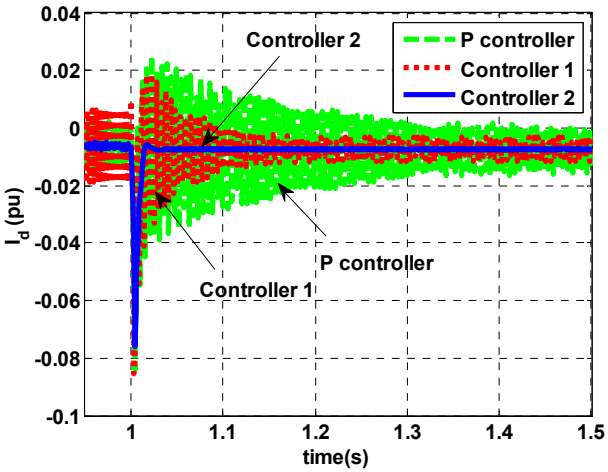

Fig. 10. Active current oscillation comparison in capacitive mode

Oscillation of I_d with the controller 2 becomes smaller quickly at both operating points. Also, it almost never oscillates at –0.8[pu]. The controller 1 has larger %OS and slower T_s than P controller at 0.8[pu]. These results can be expected through the root locus analysis as shown in Fig. 4. The absolute value of the real part of the controller 1's internal dynamics poles is much smaller than that of the P controller's when the operating point is 0.8[pu] but vice versa when the operating point is –0.8[pu]. Therefore, the controller 1 cannot always guarantee better performance than P controller. Additionally, if the reference is changed in short time then, remain oscillations will affect the next control period because of the slowed response with either controller 1 or P controller. The controller 2 shows the best performance among them at every operating point because the controller 2's internal poles are always further to the left than the ones of the P controllers and the controller 1.

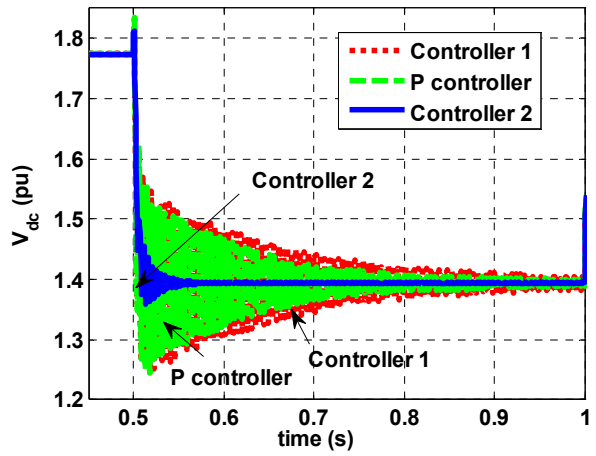

Fig. 11. DC voltage oscillation comparison in inductive mode

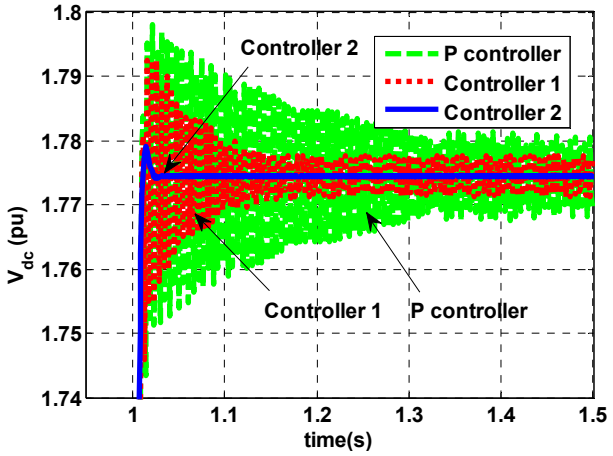

Fig. 12. DC voltage oscillation comparison in capacitive mode

Fig. 11 and Fig. 12 show the V_{dc} oscillations comparison results. The control input, α, as well as V_{dc} have same tendencies as I_d cases at each operating point. Through these results, we can confirm that the controller 2 provides improved stability of the internal dynamics apparently due to variable gain.

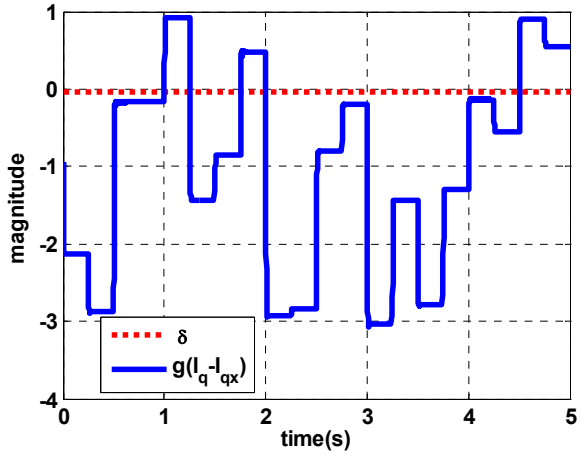

Fig. 13. Gain comparison of dI_d/dt term between controller 1 and controller 2

For arbitrary I_{qref} sequences, the gains multiplied by dI_d/dt term of the controller 1 and controller 2 are compared in Fig. 13. The gain, $g(I_q\text{-}I_{qx})$, of the controller 2 varies at each operating point while the one of the controller 1 is fixed to δ. If $g(I_q\text{-}I_{qx})$ has almost same value as δ then, the controller 2 shows less improved performance than where $g(I_q\text{-}I_{qx})$ is highly different from δ.

B. Simulation Results using a Topological Model

Performance of the proposed control scheme was also validated through simulations using a detailed topological model with power electronic devices and the detailed driving characteristics. The benchmark model is the demo model of Matlab/ Simulink SimPowerSystems toolbox: 48 pulses 100MVA STATCOM model. The parameter and structure was revised to 24 pulses 100MVA STATCOM, which will be installed at Migeum S/S. The sampling time of the controller was set to 65[us] and that of the power electronics was set to 1[us]. The controller gain of the discrete system depends on the sampling time, so the controller gain of the topological model is different from the one in the average model [16].

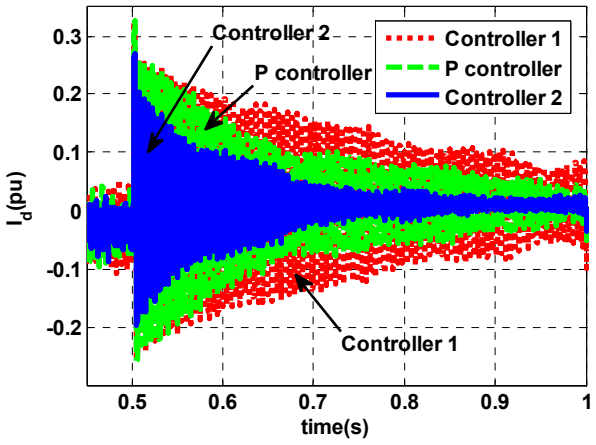

Fig. 14. Active current oscillation comparison in inductive mode (topological model)

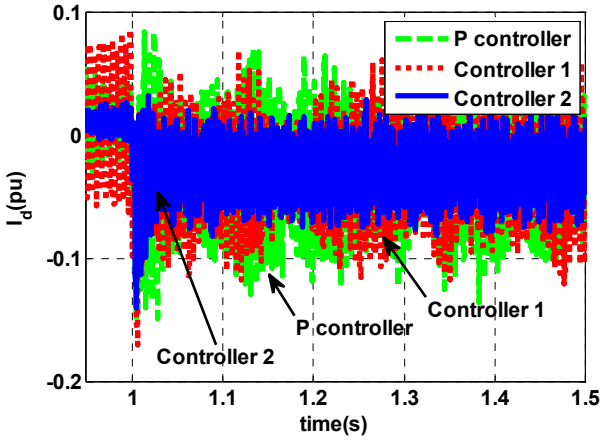

Fig. 15. Active current oscillation comparison in capacitive mode (topological model)

Fig. 14 and Fig. 15 show the results of the active current at inductive (Iqref = 0.8[pu]) and capacitive mode (Iqref = -0.8[pu]).

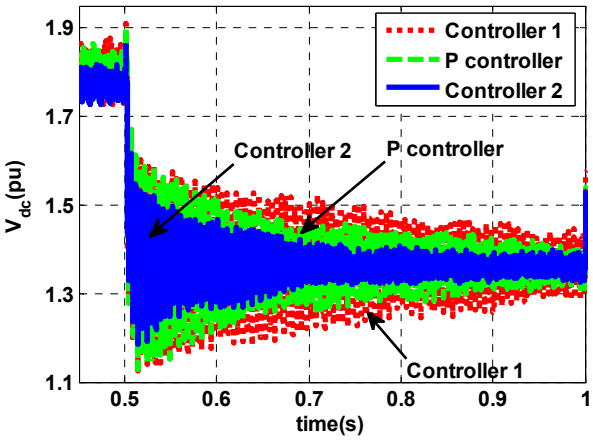

Fig. 16. DC voltage oscillation comparison in inductive mode (topological model)

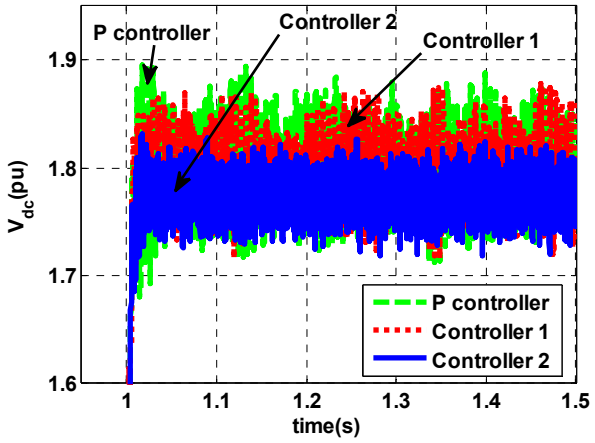

Fig. 17. DC voltage oscillation comparison in capacitive mode (topological model)

Fig. 16 and Fig. 17 show the results of the DC voltage at each mode. Settling time and %OS are not exactly the same as those of the simulation results through the averaged model. However, the results have similar tendencies in their performance order.

VII. Conclusion

A new nonlinear feedback controller based on input-output linearization is proposed for stabilization of internal dynamics in STATCOM. Through input-output linearization the nonlinearity in the system is eliminated. The proposed nonlinear feedback controller includes the derivative of the active current term with a variable gain about operating points. The improved performance was compared with the P controller and the previous nonlinear controller with constant gain. To ensure the stabilization of the internal dynamics, a root locus analysis is performed at each operating point. Its effectiveness is validated through time response properties using averaged model and topological one. The proposed controller showed improved internally stability at whole operation range. It reduced the settling time and overshoot of I_d and V_{dc}. Consequently these results resulted in the reduction of the current ripples on the DC side capacitor and less shock to the capacitor. Thus the increased lifecycle of the capacitor is expected.

VIII. Appendix

$$\Delta\dot{I}_d' = -\frac{R_s'\omega}{L'}\Delta I_q' + \omega\Delta I_q' + \frac{k\omega}{L'}\Delta V_{dc}' - \frac{\omega}{L'}\Delta v'$$

$$\Delta\dot{I}_q' = \left(-\frac{gR_s'\omega}{L'}I_{qo}' + \frac{2gR_s'\omega}{3kC'L'}V_{dc0}'\right)\Delta I_d'$$
$$+\left(2g\omega I_{qo}' + \frac{gk\omega}{L'}V_{dco}' - \frac{g\omega}{L'}v_o' - \frac{2g\omega}{3kC'}V_{dco}' - \lambda\right)\Delta I_q'$$
$$+\left(\frac{gk\omega}{L'}I_{qo}' - \frac{2g\omega}{3k'}I_{qo}' - \frac{4g\omega}{3C'L'}V_{dco}' + \frac{2g\omega}{3kC'L'}v_o'\right)\Delta V_{dc}'$$
$$+\left(-\frac{g\omega}{L'}I_{qo}' + \frac{2g\omega}{3kC'L'}V_{dco}'\right)\Delta v' + \lambda\Delta I_{qref}'$$

$$\Delta\dot{V}_{dc}' = \left\{-\frac{3kC'\omega}{2} - \frac{3C'L'\omega I_{qo}'}{2V_{dc0}'} + \frac{3gC'R_s'\omega\left(I_{qo}'\right)^2}{2V_{dco}'} - \frac{gR_s'\omega I_{qo}'}{k}\right\}\Delta I_d'$$
$$+\left\{\left(-3C'R_s'\omega + 3C'L'\lambda\right)\frac{I_{qo}'}{V_{dco}'} - \frac{9C'L'g\omega\left(I_{qo}'\right)^2}{2V_{dco}'} - \frac{3C'L'\lambda I_{qref}'}{2V_{dco}'}\right.$$
$$\left.-3C'gk\omega I_{qo}' + g\omega V_{dco}' - \frac{g\omega v_o'}{k} + \frac{3C'g\omega I_{qo}'v_o'}{V_{dco}'} + \frac{2L'g\omega I_{qo}'}{k}\right\}\Delta I_q'$$
$$+\left\{\left(\frac{3C'R_s'\omega}{2} - \frac{3C'L'\lambda}{2}\right)\cdot\left(\frac{I_{qo}'}{V_{dco}'}\right)^2 + \frac{3C'L'\lambda I_{qref}'I_{qo}'}{2\left(V_{dco}'\right)^2} - \frac{\omega C'}{R_p'}\right.$$
$$\left.+\frac{3C'L'g\omega\left(I_{qo}'\right)^3}{2\left(V_{dco}'\right)^2} - \frac{3C'g\omega v_o'\left(I_{qo}'\right)^2}{2\left(V_{dco}'\right)^2} + g\omega I_{qo}'\right\}\Delta V_{dc}'$$
$$+\left\{\frac{3C'g\omega\left(I_{qo}'\right)^2}{2V_{dco}'} - \frac{g\omega I_{qo}'}{k}\right\}\Delta v' + \left\{-\frac{3C'L'\lambda I_{qo}'}{V_{dco}'}\right\}\Delta I_{qref}'$$

IX. References

[1] "ABB STATCOM for Flexibility in Power Systems"; ABB Power Systems brochure no. A02-0-165E; ABB Västerås, Sweden

[2] Z. Yao, M. S. Dawande and V. Rajagopalan, "Controller design for advanced reactive power compensators based on input-output linearization," in *Proc. IEEE PESC'97*, vol. 2, 1997, pp. 936–941.

[3] Z. Yao, N.s Lechevin, "Issues on nonlinear control of voltage source FACTS devices," in *Proceedings of the 2005 IEEE Conference on Control Applications,* Toronto, Canada, Aug. 28-31, 2005, pp. 1317-1324.

[4] N.C.Sahoo, B.K. Panigrahi, P.K. Dashand G. Panda, "Application of a multivariable feedback linearization scheme for STATCOM control," *Electric Power Systems Research,* vol. 62, Issue 2, 28, June 2002, pp.81-91.

[5] P. Petitclair, S. Bacha, J. P. Rognon, "Averaged modeling and nonlinear control of an ASVC (Advanced Static VAR Compensator)," in IEEE PESC'96, Baveno, Italy, June 24-27, 1996, pp.753-758.

[6] P. Petitclair, S. Bacha, J-P Ferrieux, "Optimized linearization via feedback control law for a STATCOM," in *Proc. Ind. Applicat. Soc. Annu. Meeting*, Oct. 1997, pp. 880–885.
[7] P. Rao, M. L. Crow and Z. Yang, "STATCOM control for power system voltage control application," *IEEE Transaction Power Delivery*, vol. 15, no. 4, Oct. 2000.
[8] A.H._Norouzi and A. M. Sharaf, "Two control schemes to enhance the dynamic performance of the STATCOM and SSSC,*" IEEE Transactions on Power Delivery*, vol.20, no. 1, Jan. 2005.
[9] A. P. Auiar, J. P. Hespanha and P. V. Kokotovic, "Zero dynamics tracking performance limits in nonlinear feedback systems," Analysis and design of nonlinear control systems, Springer, Part3, Nov. 2007.
[10] S. Sastry, Nonlinear systems. Springer, 1999.
[11] S. Ibaraki and M. Tomizuka, "Taming internal dynamics by mismatched and H_∞−optimized state observer," *in Proceedings of the American Control Conference*, Chicago, Illinis, June, 2000, pp. 715-719.
[12] C. Schauder, M. Gernhardt, E. Stacey, T. W. Cease, A. Edris, "Development of a ±100MVAR static condenser for voltage control of transmission systems," *IEEE Transactions on Power Delivery,* vol. 10, no. 3, July 1995
[13] C. Schauder, H. Mehta, "Vector analysis and control of advanced static var compensator," in *Proc. Inst. Elect. Eng. C*, vol. 140, no. 4, pp. 299–306, July 1993.
[14] Hassan K. Khalil, *Nonlinear systems*. Prentice Hall, 3rd edition. 2002.
[15] C. Schauder, "Advanced static var compensator control system," U.S. Patent 5,329,221, July 12, 1994.
[16] G. F. Franklin, J. D. Powell and M. Workman, *Digital control of dynamic systems*. Addison-Wesley Longman Publishing Co., Inc. Boston, MA, USA 1997.

X. BIOGRAPHIES

Youngseong Han received B.S. and M.S. in electrical engineering from Hanyang University, Seoul, Korea, in 1990 and 1992, respectively and is currently studying toward Ph.D. degree in electrical engineering at Hanyang University, Seoul, Korea. He joined Hyosung Corporation in 1991. He is currently in charge of the development of FACTS equipment at Hyosung. His major research areas are STATCOM, Back to Back STATCOM and power quality equipment.

Young Ok Lee was born in Seoul, Korea, on 29 September 1983. She received the B.S. degree in electrical and computer engineering from the Hanyang University, Seoul, Korea, in 2002. She is currently in the Ph.D. program at the same university. Her current research focuses on the nonlinear control of power system and vehicle brake system.

Chung Choo Chung 5 September 1958. He received the B.S. and M.S. degrees from Seoul National University in 1981 and 1983, respectively, and the Ph.D. degree from the University of Southern California in 1993, all in Electrical Engineering. He was a Research Engineer at Central Research Laboratory, GoldStar (Former LG Electronics), Seoul, Korea from 1983 to 1985, where he worked in the area of robot control and copier. He joined International Procurement Office, IBM Korea in 1985 and worked as Procurement and Quality Assurance Engineer until 1987. From 1993 to 1994, he was a Research Associate in Electrical and Computer Engineering at the University of Colorado at Boulder, U.S.A. From 1994 to 1997, he was with Samsung Advanced Institute of Technology, Korea where he was a team leader developing a disk drive servo development system. He was appointed as a member of 21 Century Leaders of Samsung Group and finished Samsung Advanced Management Program at Wharton Business School, U.S.A. in 1996. In 1997 he joined the faculty of Hanyang University. Currently he is a Professor in Electrical and Biomedical Engineering. Dr. Chung served as an Associate Editor for the Asian Journal of Control (AJC) from 2000 to 2002 and Director of Editorial Board for the Transactions on Control, Automation and Systems Engineering from 2001 to 2002. Also he served as an Editor for the International Journal of Control, Automation and Systems (IJCAS) from 2003 to 2005. He served as an Associate Editor for 2003 IEEE Conference on Decision and Control. Since 2000, he has been president of Control Theory Study Society of ICASE, Korea. He was a Publicity Chair of 2008 IFAC World Congress in Seoul, Korea. He is Co-Program Chair, ICCAS-SICE 2009, in Japan. His current research interests are in the areas of nonlinear control theory, robotic system, vehicle dynamics control and data storage systems, and stability problem of electric power system.